Journal Pre-proof

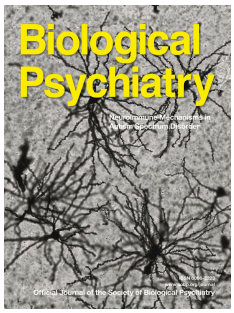

Noninvasive modulation of subcallosal cingulate and depression with focused ultrasonic waves

Thomas S. Riis, Daniel A. Feldman, Sarah S. Kwon, Lily C. Vonesh, Vincent Koppelmans, Jefferson R. Brown, Daniela Solzbacher, Jan Kubanek, Brian J. Mickey

PII: S0006-3223(24)01662-7

DOI: https://doi.org/10.1016/j.biopsych.2024.09.029

Reference: BPS 15622

To appear in: *Biological Psychiatry*

Received Date: 5 May 2024

Revised Date: 19 September 2024

Accepted Date: 30 September 2024

Please cite this article as: Riis T.S., Feldman D.A., Kwon S.S., Vonesh L.C., Koppelmans V., Brown J.R., Solzbacher D., Kubanek J. & Mickey B.J., Noninvasive modulation of subcallosal cingulate and depression with focused ultrasonic waves, *Biological Psychiatry* (2024), doi: https://doi.org/10.1016/j.biopsych.2024.09.029.

Noninvasive modulation of subcallosal cingulate and depression with focused ultrasonic waves

Thomas S. Riis*[a], Daniel A. Feldman*[a,b,c], Sarah S. Kwon[c], Lily C. Vonesh[c], Vincent Koppelmans[c], Jefferson R. Brown[c], Daniela Solzbacher[c], Jan Kubanek*[a,c], Brian J. Mickey*[a,c]

[a]*Department of Biomedical Engineering, University of Utah, Salt Lake City, UT, United States*
[b]*Department of Radiology, University of Utah, Salt Lake City, UT, United States*
[c]*Department of Psychiatry, Huntsman Mental Health Institute, University of Utah, Salt Lake City, UT, United States*

* Contributed equally

Correspondence:

Brian J. Mickey, MD, PhD
brian.mickey@utah.edu
501 Chipeta Way, Salt Lake City, UT 84108
801-587-3297

Thomas S. Riis, PhD
tom.riis@utah.edu
36 S. Wasatch Drive, SMBB 3100, Salt Lake City, UT 84112
801-581-8528

Short/running title: Ultrasonic neuromodulation of subcallosal cingulate

Keywords: ultrasound, deep brain stimulation, neuromodulation, subgenual cingulate, subcallosal cingulate, depression

Abstract

Background: Severe forms of depression have been linked to excessive subcallosal cingulate (SCC) activity. Stimulation of SCC with surgically implanted electrodes can alleviate depression, but current noninvasive techniques cannot directly and selectively modulate deep targets. We developed a new noninvasive neuromodulation approach that can deliver low-intensity focused ultrasonic waves to the SCC. *Methods:* Twenty-two subjects with treatment-resistant depression participated in a randomized, double-blind, sham-controlled study. Ultrasonic stimulation was delivered to bilateral SCC during concurrent functional MRI to quantify target engagement. Mood state was measured with the Sadness subscale of the Positive and Negative Affect Schedule before and after 40 minutes of real or sham SCC stimulation. Change in depression severity was measured with the 6-item Hamilton Depression Rating Scale (HDRS- 6) at 24 hours and 7 days. *Results:* Functional MRI demonstrated a target-specific decrease in SCC activity during stimulation (p=0.028, n=16). In 7 of 16 participants, SCC neuromodulation was detectable at the individual-subject level with a single 10-minute scan (p<0.05, small-volume-correction). Mood and depression scores improved more with real than with sham stimulation. In the per-protocol sample (n=19), real stimulation was superior to sham for HDRS-6 at 24 hours and for Sadness (both p<0.05, d>1). Non-significant trends were found in the intent-to-treat sample. *Conclusions:* This small pilot study indicates that ultrasonic stimulation modulates SCC activity and can rapidly reduce depressive symptoms. The capability to noninvasively and selectively target deep brain areas creates new possibilities for future development of circuit-directed therapeutics, and for the dissection of deep-brain circuit function in humans.

https://clinicaltrials.gov/study/NCT05301036

Introduction

Deep neural circuits are implicated in the pathophysiology of numerous psychiatric illnesses including mood disorders, anxiety disorders, and addictions. Current treatments for these illnesses are often ineffective, but better therapeutic approaches may be possible through specific and precise modulation of the activity of deep neural targets. Severe depression, for example, has been linked to excessive activity of the subcallosal cingulate cortex (SCC), a limbic region situated ventral to the corpus callosum (1). Functional imaging studies (1–4) have shown that the SCC is hyperactive in depressed individuals and interventional studies (5–8) indicate that disruption of SCC activity by deep brain stimulation can relieve depressive symptoms.

Current approaches to deep brain stimulation, however, require surgical implantation of stimulation leads, which carry considerable risks (9) and high costs that limit the spectrum of individuals who could benefit. Current noninvasive neuromodulation modalities, on the other hand, are limited in other ways. Transcranial magnetic and electric stimulation cannot directly and selectively modulate deep structures like the SCC due to fundamental physical limitations of electromagnetic fields. This lack of selectivity leads to limited effectiveness and excessive adverse effects.

To address these limitations, we have developed an approach and a device that can modulate the SCC and other deep targets noninvasively and precisely (10–13). The device uses ultrasound transducer arrays to focus low-intensity ultrasonic waves into deep brain targets through the intact skull and scalp (11). Critically, the device measures and compensates for the substantial aberrations of ultrasound by the human head, thus delivering into the target a controlled, deterministic, and safe ultrasound intensity (10).

Here, we applied this new approach to a cohort of participants with treatment-resistant depression using a randomized, blinded, sham-controlled study design. Ultrasonic stimulation was delivered to the SCC using individualized MRI guidance, and the neural effects of stimulation were quantified using concurrent functional MRI. The two parallel objectives of the study were (1) to demonstrate that ultrasonic stimulation engages the SCC target and (2) to characterize the immediate mood effects and tolerability of this stimulation. We hypothesized that SCC sonication would deactivate SCC and improve mood and depressive symptoms.

Methods and Materials

Study Design and Participants

This study was approved by the University of Utah Institutional Review Board, monitored by an independent safety monitor, and pre-registered on clinicaltrials.gov (NCT05301036). All subjects provided written informed consent. Eligible individuals were adults (age 18-65 years) with a primary DSM-5 diagnosis of major depressive disorder or bipolar disorder and a current moderate-to-severe depressive episode without psychotic features lasting at least 2 months (see Supplementary **Table S1** for full inclusion/exclusion criteria). This pilot study incorporated a double-blind, randomized, sham-controlled, cross-over design (**Fig. 1**). Clinical evaluation was performed at the baseline visit, and approximately 1 week later the participant returned for the first stimulation visit, where they were randomized 1:1 to the real-stimulation or sham-stimulation arm. At the first stimulation visit, each subject participated in a 1-hour MRI session followed immediately by a 1-hour treatment session. Seven days later, each participant returned for the second stimulation visit, where subjects crossed over from real to sham, or sham to real. At the second stimulation visit, the 1-hour MRI session and 1-hour treatment session were repeated. Symptoms were assessed at the start and end of each stimulation visit, and 24 hours and 7 days following each stimulation visit. The prespecified enrollment target was 20 subjects with analyzable data. As shown in **Suppl. Fig. S1**, 29 subjects were enrolled, 22 were randomized, and 20 crossed over. The two subjects described previously (10–12) are not included in this report.

Ultrasound Device

The ultrasound device and approach are fully described in the Supplemental Methods and recent publications (11, 10). Briefly, two ultrasound transducer phased arrays were situated in a frame over the left and right sides of the head. Acoustic coupling gels were placed between each array and the head, and a thermoplastic mask was individually fit to the participant's head to minimize movement relative to the frame and transducer arrays. A transmit-receive scan was performed between the two arrays to measure the acoustic distortion caused by the head and coupling, and an algorithm calculated phase and amplitude adjustments at each transducer element that fully compensated for the distortion. MRI was performed with the ultrasound transducer arrays locked in place and the arrays were coregistered to the individual's brain anatomy using fiducial markers on the device that were visible in the MRI. The device created a sonication focus that extended 20.4 mm x 2.4 mm x 3.6 mm (x, y, z dimensions in Montreal Neurological Institute

(MNI) space). The focus was moved to the desired target programmatically without moving the device or subject. To assure safety, ultrasound intensities were always delivered below the FDA 510(k) Track 3 guidelines for diagnostic ultrasound (peak intensity < 190 W/cm^2, time-averaged intensity < 720 mW/cm^2, mechanical index < 1.9) ((14)).

Targeting and Measurement of Target Engagement

The individual's T1-weighted image was used to guide ultrasound targeting. Blood oxygenation level dependent (BOLD) imaging was used to measure target engagement. Details of MRI acquisition are provided in the Supplementary Methods. The center of the sonication focus was positioned on the midline, spanning left and right SCC, in order to approximate bilateral targets previously described for invasive DBS (15). Individual targets are shown in **Suppl. Fig. S2**. Ultrasound was delivered with amplitude of 1 MPa at target (31.1 W/cm^2; following skull correction (10)), 30 ms burst duration containing pulses of 5 ms on and 5 ms off, separated by 1.4-second burst intervals, for 60 seconds. These stimulus parameters were expected to cause net inhibitory effects (16, 17). Neuromodulation was quantified using concurrent (online) BOLD imaging with a 10-minute block-design paradigm consisting of five 1-minute rest epochs (no sonication) interleaved with five 1-minute epochs of active sonication. Continuous white noise was played throughout the 10-minute session via earbuds with the goal of masking any potential auditory effects caused by the ultrasound. Because of technical difficulties during some BOLD imaging sessions, in several cases it was necessary to deviate from protocol and repeat real stimulation during functional MRI at the second stimulation session even though treatment assignment had crossed over from real to sham (see Supplemental Methods). Usable BOLD data were not obtainable from 5 of 21 participants who received sonication during MRI due to technical problems, so the final data set reported here includes a total of 16 subjects.

Randomization and Blinding

Participants were randomized to real (active) or sham (placebo) groups when they arrived for the first stimulation visit. The device operator was necessarily unblinded to allocation at the first stimulation visit. All other staff, participants, and clinical raters remained blinded. Treatment allocation was disclosed to participants following the HDRS-6 rating, 7 days after the second stimulation visit. The effectiveness of blinding was assessed by asking a subset of 13 participants to guess which intervention they received. See Supplemental Methods for details.

Real and Sham Treatment Sessions

Immediately after MRI with concurrent stimulation, additional stimulation was delivered outside the scanner during a single 1-hour treatment session including 39-41 minutes (cumulative) of real or sham sonication (**Fig. 1**). Because the optimal target was not known with millimeter precision, three adjacent midline targets within the SCC region were stimulated sequentially, with the goal of maximizing changes in mood symptoms. In addition to the original target stimulated during concurrent functional MRI, two targets approximately 4 mm anterior and 4 mm posterior were defined on the individual MRI. These three SCC targets (anterior, middle, posterior) were then stimulated for equal duration, in random order, over a 1-hour session. Ultrasound was delivered to each target with amplitude of 1 MPa (31.1 W/cm^2; following skull correction (10)), with 30-ms burst duration containing pulses of 5 ms on and 5 ms off, separated by 1.4- or 0.7-second burst intervals. Overall, the treatment session consisted of 3 blocks (A, B, C), each of which included stimulation of all three targets. Block A contained 3-5 one-minute sonications to test the tolerability of each target with 1.4-second burst intervals. Block B contained 6 three-minute sonications with 1.4-second burst intervals. Block C contained 6 three-minute sonications with 0.7-second burst intervals.

To mask the faint vibratory percepts sometimes experienced with ultrasound stimulus delivery (18, 19), subjects wore earbuds and received identical auditory stimuli during both active and sham interventions. White noise was combined with audio recordings of ultrasound pulses from the arrays, and auditory stimuli were timed to coincide with delivery of ultrasound stimulation.

Clinical Outcome Measures

Two co-primary efficacy measures were pre-specified. The Sadness sub-scale of the expanded Positive and Negative Affect Schedule (PANAS-X) quantified immediate change in mood state, and the HDRS-6 measured changes in depressive symptom severity at 24 hours and 7 days (see **Fig. 1)**. The PANAS-X is a reliable, validated, 60-item, self-report of mood state (20). The HDRS-6 is an abbreviated version of the original 17-item instrument (21) that correlates with longer versions of the HDRS, is sensitive to change, and unlike the 17-item scale can be applied to brief time frames allowing measurement of rapid effects (22–25). Tolerability and safety were assessed at each visit through collection of spontaneously reported adverse events, the General Assessment of Side Effects (GASE) scale (26), the YMRS, and the C-SSRS. Secondary outcomes included the self-reported Inventory of Depressive Symptomatology (IDS-SR) and 7-item Generalized Anxiety Disorder scale (GAD-7). Details are described in the

Supplementary Material.

Functional MRI Analysis

The functional MRI processing pipeline is described in the Supplementary Methods. Whole-brain data from a single 10-minute scan was analyzed for each subject using a standard first-level SPM12 general linear model (GLM). The first-level model employed a block design that contrasted five 1-minute *ON* epochs (active ultrasonic stimulation) versus five 1-minute *OFF* epochs (no stimulation). Fitting of this model produced whole-brain beta-weight maps for *ON>OFF* and *OFF>ON*, as well as corresponding *t* statistic maps, at each voxel.

The primary analysis of target engagement used a region of interest (ROI) corresponding to the SCC volume where ultrasound was delivered (described in the Supplementary Methods). To evaluate target engagement for each subject, SPM12 family-wise-error small-volume-correction (FWE-SVC) was applied to the subject's *t* statistic maps (*ON>OFF* and *OFF>ON*) using the SCC ROI. This produced one-tailed *p* values for activation (*ON>OFF*) and deactivation (*OFF>ON*) of the SCC for that subject. A threshold of $p < 0.025$ for either activation or deactivation was considered significant (equivalent to a single two-tailed *t*-test with a conventional threshold of $p < 0.05$). To evaluate target engagement at a group level, a second-level *ON>OFF* group model was constructed and collapsed beta-weights were extracted from the SCC ROI for each participant. A two-tailed one-sample *t*-test was applied to these extracted beta-weights and $p < 0.05$ was considered significant. Analysis of brain-wide effects is described in the Supplemental Methods.

Analysis of Clinical Outcomes

Change in PANAS-X Sadness (post- minus pre-stimulation) at the first stimulation visit was calculated for each subject and the difference between treatment groups (real versus sham) was evaluated using a two-sample t-test. Similarly, changes in HDRS-6 score 24 hours and 7 days after the first stimulation visit were calculated, and two-sample t-tests were applied to test for group differences at each time point.

The intention-to-treat sample included all 22 participants who were randomized. The per-protocol sample (n = 19) excluded 3 subjects who received stimulation other than as intended in the pre-specified protocol. One participant had received active stimulation during MRI under a different protocol prior to being randomized to the real arm; one received active stimulation during MRI despite being randomized to the sham arm; and one inadvertently received

several minutes of active stimulation during the sham treatment session.

Results

Characteristics of Participants

Twenty-nine adults with treatment-resistant depression enrolled in the study and 22 were randomized (see CONSORT diagram, **Suppl. Fig. S1**). Ten were assigned real stimulation at the first session and 12 sham stimulation. Demographic and clinical characteristic were comparable for real- versus sham-stimulation groups (all $p > 0.05$, **Table 1**). Twenty participants returned for a second stimulation visit to cross over to the other condition (sham or real).

Target Engagement

Individual-level analyses showed statistically significant neuromodulation in the targeted SCC region in 7 of 16 subjects ($p < 0.05$, FWE-SVC) based on a single 10-minute BOLD imaging session (**Suppl. Table S2**). For 5 subjects, the expected decrease in BOLD signal (i.e., deactivation) was detected. An example of the SCC deactivation is shown in **Fig. 2*A*-*C***. Nine participants showed no significant modulation and 2 showed significant activation of the SCC. At the group level, the average effect of the SCC modulation was deactivation: beta-weights extracted from the SCC region of interest (**Fig. 2*D***) were significantly less than zero across the cohort ($t(15) = -2.43$, $p = 0.028$, one-sample two-tailed t-test).

Brain-wide Effects

To evaluate the broader effects of SCC modulation on brain networks, we evaluated the effects across the brain in each subject. Diverse patterns of activation and deactivation were observed in distributed brain regions (**Suppl. Fig. S3**). At the group level, whole-brain analysis revealed no consistent deactivation beyond the SCC ($p > 0.05$, false discovery rate corrected). However, activation (i.e., an increase in activity) was detected at a group level in the left ventrolateral prefrontal cortex and right superior temporal gyrus (**Suppl. Table S3**).

Responses in distributed brain areas may depend on the polarity of the SCC modulation. We therefore also analyzed the subset of the 12 subjects for whom sonication deactivated the SCC. Significant deactivation was found only in the SCC (**Fig. 3**). Activation was detected in the left ventrolateral prefrontal cortex and bilateral temporal

cortex (**Suppl. Table S3**), in line with the findings for the full cohort.

Changes in Mood and Depression

The primary efficacy endpoints were change in PANAS-X Sadness immediately following stimulation, and change in HDRS-6 score 24 hours and 7 days following the stimulation visit.

In the per-protocol sample (n = 19), the group difference for change in Sadness was statistically significant (p = 0.027, $t(16) = -2.43$, $d = -1.15$), as shown in **Fig. 4**. Pre-treatment Sadness scores were higher for the real-stimulation group than for the sham-stimulation group (56.1 versus 39.5) but the difference was not statistically significant; post-treatment Sadness scores also did not differ by treatment group (**Suppl. Table S5**).

In the per-protocol sample, change in HDRS-6 was significant at 24 hours (p = 0.031, $t(17) = -2.35$, $d = -1.08$) but not at 7 days (p = 0.22, $t(17) = -1.29$, $d = -0.59$), as shown in **Fig. 5**. The rate of response (improvement ≥ 50% in HDRS-6) for sham versus active stimulation was 20% versus 67% at 24 hours, and 30% versus 67% at 7 days (**Fig. 5*E***).

For the intent-to-treat sample (n = 22), scores decreased more in the real-stimulation group compared with the sham-stimulation group, but group differences did not reach a $p < 0.05$ significance for Sadness (p = 0.064, $t(19) = -1.96$, Cohen's $d = -0.87$), HDRS-6 at 24 hours (p = 0.18, $t(20) = -1.38$, $d = -0.59$), or HDRS-6 at 7 days (p = 0.45, $t(20) = -0.77$, $d = -0.33$).

Tolerability and Safety

During this cross-over study, 21 participants received real stimulation and 21 received sham stimulation. No serious adverse events (SAEs) occurred during the course of the study. No severe adverse events occurred during or immediately after stimulation. No subjects experienced mania or hypomania.

At follow-up visits 24 hours after each stimulation visit, self-reported side effects were collected with a standardized questionnaire (**Table 2**). The symptoms most commonly reported were depressed mood (real, 62%; sham 67%), headache (real, 57%; sham, 67%), and anxiety (real, 57%; sham 52%). Suicidal thoughts were reported by 29% of subjects after real stimulation and 24% of subjects after sham.

Two participants experienced a severe psychiatric adverse event with onset later than the 24-hour follow-up visit,

both of which followed real stimulation. The first participant developed acute depression with suicidal ideation 3 days after stimulation and took an intentional overdose of medication that did not require medical intervention. The other subject developed rapid worsening of depression with suicidal ideation a few hours after the 24-hour follow-up visit. Both subjects had a history of similar mood swings in the past. Over the subsequent 2 weeks, depression improved and suicidal ideation resolved for both participants.

Effectiveness of Blinding

At the end of the first stimulation visit, 13 participants were asked to guess which intervention they received on a 0–100 scale, 50 representing complete uncertainty. The mean (SD) rating was 48 (32) for the sham group and 64 (26) for the active group. Neither was significantly different from 50 ($p = 0.87$ and $p = 0.30$, one-sample two-tailed t-tests), and mean values for the two groups did not differ from each other ($p = 0.35$, two-sample two-tailed t-test). This suggests that the blinding procedures used in this study were effective.

Discussion

Here we report the first application of a novel neuromodulation approach to a cohort of individuals with treatment-resistant depression. In this approach, a phased array device delivers ultrasound into specified deep brain targets, while measuring and compensating for the severe aberrations of ultrasound by the head (10, 11). We found that transcranial delivery of low-intensity focused ultrasound to the SCC can safely reduce SCC activity, elicit immediate mood improvement, and rapidly decrease depressive symptoms. This proof-of-principle demonstration suggests that this approach could be developed into an effective, noninvasive, rapidly acting intervention for depression. More generally, the capability to noninvasively, flexibly, and selectively target deep brain areas creates new possibilities for circuit-directed therapeutic interventions for a range of neuropsychiatric disorders.

Precise and noninvasive modulation of deep brain targets in humans has been an elusive goal. Ultrasonic energy has become a prime candidate for attaining this objective (27–29). Ultrasonic waves combine a unique triad of properties—noninvasiveness, depth penetration, and sharp focus. Compared to electromagnetic waves, sound waves have a small wavelength. Thanks to diffraction (30), the short wavelength enables relatively sharp focus at depth. Nonetheless, ultrasonic technology has been impeded by formidable barriers—the skull and hair, which attenuate and distort ultrasonic waves severely and unpredictably (31, 10). The approach used here directly measures and compensates for these barriers in each individual, thus delivering into specified targets a controlled, deterministic ultrasound intensity, resulting in safe and effective neuromodulation (10, 11, 13).

We hypothesized that sonication of the SCC would reduce activity in the targeted area. This result was confirmed for the group as a whole and for five subjects with statistically significant deactivation at the individual level (**Fig. 2*D***). However, we also observed substantial inter-individual variability, with two subjects showing significant activation of SCC during sonication. Potential sources for this variability include imperfect correction of ultrasound aberration by the device, millimeter-scale variation in targeting, and individual anatomical or physiological differences. The latter possibility has been highlighted by invasive deep brain stimulation experiments which indicate that individual tractography may be necessary for optimal placement of electrodes(32). Similar individualized optimization of targeting may be needed with noninvasive focused ultrasound to achieve consistent effects across subjects. A major advantage of our method over surgical approaches is that the ultrasound focus is readily steered to a different target without moving the device or subject. Furthermore, multiple targets can be defined and sonicated

sequentially or near-simultaneously. The flexibility of this approach, along with the safety of repeated stimulation, lends itself well to individualized optimization. This flexible approach could also be applied to other targets investigated with surgical deep brain stimulation such as the medial forebrain bundle and the ventral striatum (6, 7). Furthermore, this noninvasive approach could have potential as a predictive pre-surgical probe for more refractory patients who are candidates for invasive deep brain stimulation.

Our findings support the idea that deactivation of the SCC with transcranial ultrasound can cause an immediate decrease in sad mood and a rapid improvement of depressive symptoms among individuals with moderate-to-severe treatment resistant depression. The differences between active and sham treatment groups were greatest for participants treated per protocol, and for the immediate and 24-hour assessments, but durable antidepressant effects lasting 1 week or longer were observed for a subset of participants. Our approach can be compared to previous studies that used single-element transducers to deliver transcranial ultrasound to the frontal lobe with the goal of modulating mood states in individuals with chronic pain (33), in healthy participants(34), and in subjects with mild-to-moderate depression(35). Those studies showed limited effectiveness and effect duration. Our approach differs from these previous studies in three fundamental ways: 1) we measured and corrected for the ultrasound aberrations by the head (10); 2) we focused the ultrasound into the target using phased arrays, which provide focal, precise, and flexible ultrasound delivery (11–13); and 3) we used MRI for guidance and BOLD imaging to validate target engagement. These approaches enabled us to deliver ultrasound into the SCC precisely, selectively, and in a controlled manner. Additional factors, such as the stimulation parameters, targeted structures, and patient profiles, may also contribute to these marked differences.

We found good overall tolerability of SCC sonication and no serious adverse events (SAEs). No severe problems were observed during or within 24 hours of stimulation, but two subjects experienced significant mood swings in the period 24-72 hours following real SCC stimulation, including clinically significant worsening of suicidal ideation, which resolved over the subsequent 2 weeks. These observations raise the possibility that SCC sonication could elicit delayed psychiatric adverse effects in some individuals. The assessment of causality is complicated by the late onset of these events following stimulation and the lack of adverse clinical response during the first 24 hours. Both participants described a history of similar seemingly unprovoked mood swings in the past. The clinical worsening seen following stimulation therefore might have been coincidental, but perhaps more likely, the ultrasonic stimulation or other study procedures triggered neural changes that required 24-72 hours to fully manifest. Future studies should

monitor the psychiatric status of participants frequently during the week following SCC stimulation.

The current study has several caveats and limitations. First, this pilot study of 22 participants was powered to detect only large effects. Medium-sized but still important effects on target engagement or clinical outcomes were likely missed and small studies such as this pose a risk of inflated effect-size estimation. Furthermore, small samples are vulnerable to random-chance imbalances in baseline characteristics between groups (such as we observed with pre-treatment Sadness scores) which can be a source of confounding. Second, as in previous studies in humans, we used auditory masking. Our functional MRI findings indicate that auditory cortex is activated bilaterally with active stimulation, consistent with anecdotal reports from subjects of auditory percepts associated with sonication. Our evaluation of the effectiveness of blinding suggested that subjects were unable to determine which intervention they received, but future studies should verify and optimize the auditory masking protocol, and directly compare real versus sham interventions also using functional MRI. Third, the cross-over study design limited the formal evaluation of subjects to only 7 days following a stimulation session. In a recent case report, we described a subject with treatment resistant depression who unexpectedly experienced remission lasting more than 6 weeks (12). Given this finding, systematic studies are needed to evaluate the effect duration over a period of many weeks to optimize the development of practical and effective clinical interventions. Fourth, targeting for this study used only T1-weighted MRI. Previous work on optimization of SCC DBS has shown that targeting differences of a few millimeters can produce diverse therapeutic effects and, furthermore, that DBS electrodes are more effective when they engage SCC structural connections (32). In future work, we plan to employ tractography in order to optimize SCC targeting. Finally, in this study we used functional MRI to evaluate target engagement; future studies would benefit from confirmation of ultrasound targeting using mechanical or elastographic methods (41, 42).

In conclusion, we provide proof-of-concept evidence that ultrasound can noninvasively modulate deep brain circuits and rapidly improve depressive symptoms. Moreover, this flexible approach offers a new diagnostic and scientific tool to dissect human neural circuitry.

Acknowledgements

We thank staff at the Imaging and Neurosciences Center for expert help with MRI acquisition; Courtney Rada for assistance collecting clinical information; and our participants for volunteering for this study. This work was supported by the NIH (R00NS100986, RF1NS128569, S10OD026788, UL1TR002538, R61MH134943), the University of Utah Col- lege of Engineering seed grant, the University of Utah Ascender grant, and the University of Utah Department of Psychiatry.

Disclosures

J.K. is an inventor on a patent related to the ultrasound device and reports a significant financial interest with SPIRE Therapeutic, which licenses the intellectual property. J.R.B. reports a family member with a significant financial interest with SPIRE Therapeutic. B.J.M. has received research support from LivaNova and Health Rhythms in the past 2 years. All other authors report no biomedical financial interests or potential conflicts of interest.

Supplement Description:

Supplemental Methods and Results, Figures S1-S3, Tables S1-S6

References

[1] C. Hamani, H. Mayberg, S. Stone, A. Laxton, S. Haber, A. M. Lozano, The subcallosal cingulate gyrus in the context of major depression, Biological psychiatry 69 (4) (2011) 301–308.

[2] D. A. Seminowicz, H. S. Mayberg, A. R. McIntosh, K. Goldapple, S. Kennedy, Z. Segal, S. Rafi-Tari., Limbic-frontal circuitry in major depression: A path modeling metanalysis, NeuroImage 22 (1) (2004) 409–418. doi:10.1016/j.neuroimage.2004.01.015.

[3] W. C. Drevets, J. Savitz, M. Trimble, The subgenual anterior cingulate cortex in mood disorders., CNS spectrums 13 (8) (2008) 663–681. doi:10.1017/s1092852900013754.

[4] L. S. Morris, S. Costi, A. Tan, E. R. Stern, D. S. Charney, J. W. Murrough, Ketamine normalizes subgenual cingulate cortex hyper-activity in depression, Neuropsychopharmacology 45 (6) (2020) 975–981.

[5] M. T. Berlim, A. McGirr, F. Van den Eynde, M. P. A. Fleck, P. Giacobbe, Effectiveness and acceptability of deep brain stimulation (DBS) of the subgenual cingulate cortex for treatment-resistant depression: A systematic review and exploratory meta-analysis, Journal of Affective Disorders 159 (2014) 31–38. doi:10.1016/j.jad.2014.02.016.

[6] M. Figee, P. Riva-Posse, K. S. Choi, L. Bederson, H. S. Mayberg, B. H. Kopell, Deep brain stimulation for depression, Neurotherapeutics 19 (4) (2022) 1229–1245.

[7] K. A. Johnson, M. S. Okun, K. W. Scangos, H. S. Mayberg, C. de Hemptinne, Deep brain stimulation for refractory major depressive disorder: a comprehensive review, Molecular Psychiatry (2024) 1–13.

[8] H. S. Mayberg, A. M. Lozano, V. Voon, H. E. McNeely, D. Seminowicz, C. Hamani, et al., Deep brain stimulation for treatment-resistant depression, Neuron 45 (5) (2005) 651–660.

[9] A. J. Fenoy, R. K. Simpson, Risks of common complications in deep brain stimulation surgery: management and avoidance, Journal of neurosurgery 120 (1) (2014) 132–139.

[10] T. Riis, D. Feldman, B. Mickey, J. Kubanek, Controlled noninvasive modulation of deep brain regions in humans, Communications Engineering 3 (1) (2024) 13.

[11] T. Riis, D. Feldman, A. Losser, B. Mickey, J. Kubanek, Device for multifocal delivery of ultrasound into deep brain regions in humans, IEEE Transactions on Biomedical Engineering (2023).

[12] T. S. Riis, D. A. Feldman, L. C. Vonesh, J. R. Brown, D. Solzbacher, J. Kubanek, B. J. Mickey, Durable effects of deep brain ultrasonic neuromodulation on major depression: a case report, Journal of Medical Case Reports 17 (1) (2023) 449. doi: 10.1186/s13256-023-04194-4

[13] T. Riis, P. Moretti, A. Losser, P. Kassavetis, J. Kubanek, Noninvasive modulation of essential tremor with focused ultrasonic waves, Journal of Neural Engineering (2024). doi:10.1088/1741-2552/ad27ef

[14] G. Darmani, T. O. Bergman, K. Butts Pauly, C. F. Caskey, L. de Lecea, A. Fomenko, et al., Non-invasive transcranial ultrasound stimulation for neuromodulation, Clinical Neurophysiology 51 (3) (2022). doi:10.1016/j.clinph.2021.12.010.

[15] P. Riva-Posse, K. S. Choi, P. E. Holtzheimer, C. C. McIntyre, R. E. Gross, A. Chaturvedi, et al., Defining critical white matter pathways mediating successful subcallosal cingulate deep brain stimulation for treatment-resistant depression., Biological psychiatry 76 (12) (2014) 963–969. doi:10.1016/j.biopsych.2014.03.029.

[16] H. Zhang, Y. Zhang, M. Xu, X. Song, S. Chen, X. Jian, et al., The effects of the structural and acoustic parameters of the skull model on transcranial focused ultrasound, Sensors 21 (17) (2021) 5962.

[17] C. Sarica, J.-F. Nankoo, A. Fomenko, T. Grippe, K. Yamamoto, N. Samuel, et al., Human Studies of Transcranial Ultrasound neuromodulation: A systematic review of effectiveness and safety, Brain Stimulation 15 (2022). doi:10.1016/j.brs.2022.05.002.

[18] V. Braun, J. Blackmore, R. O. Cleveland, C. R. Butler, Transcranial ultrasound stimulation in humans is associated with an auditory confound that can be effectively masked, Brain Stimulation 13 (2020) 1527–1534. doi:10.1016/j.brs.2020.08.014.

[19] K. Zeng, G. Darmani, A. Fomenko, X. Xia, S. Tran, J.-F. Nankoo, et al., Induction of human motor cortex plasticity by theta burst transcranial ultrasound stimulation, Annals of Neurology 91 (2022) 238–252. doi:10.1002/ana.26294. URL https://onlinelibrary.wiley.com/doi/abs/10.1002/ana.26294

[20] D. B. Watson, L. A. Clark, The PANAS-X manual for the positive and negative affect schedule, no. May, 1994, p. 28. URL https://api.semanticscholar.org/CorpusID:17751759

[21] M. Hamilton, A rating scale for depression., Journal of neurology, neurosurgery, and psychiatry 23 (1) (1960) 56–62. doi:10.1136/ jnnp.23.1.56.

[22] P. Bech, P. Allerup, L. F. Gram, N. Reisby, R. Rosenberg, O. Jacobsen, et al., The Hamilton depression scale. Evaluation of objectivity using logistic models., Acta Psychiatrica Scandinavica 63 (3) (1981) 290–299. doi:10.1111/j.1600-0447.1981.tb00676.x.

[23] R. L. O'Sullivan, M. Fava, C. Agustin, L. Baer, J. F. Rosenbaum, Sensitivity of the six-item Hamilton

Depression Rating Scale., Acta Psychiatrica Scandinavica 95 (5) (1997) 379–384. doi:10.1111/j.1600-0447.1997.tb09649.x.
[24] B. W. Dunlop, S. V. Parikh, A. J. Rothschild, M. E. Thase, C. DeBattista, C. R. Conway, et al., Comparing sensitivity to change using the 6-item versus the 17-item Hamilton depression rating scale in the GUIDED randomized controlled trial., BMC psychiatry 19 (1) (2019) 420. doi:10.1186/s12888-019-2410-2.
[25] A. J. Rush, C. South, S. Jain, R. Agha, M. Zhang, S. Shrestha, et al., Clinically significant changes in the 17- and 6-item hamilton rating scales for depression: A star*D report, Neuropsychiatric Disease and Treatment 17 (4) (2021) 2333–2345. doi:10.2147/NDT.S305331.
[26] W. Rief, A. J. Barsky, J. A. Glombiewski, Y. Nestoriuc, H. Glaesmer, E. Braehler, Assessing general side effects in clinical trials: reference data from the general population, Pharmacoepidemiology and drug safety 20 (4) (2011) 405–415.
[27] O. Naor, S. Krupa, S. Shoham, Ultrasonic neuromodulation, Journal of Neural Engineering 13 (3) (2016) 031003.
[28] J. Kubanek, Neuromodulation with transcranial focused ultrasound, Neurosurgical Focus 44 (2) (2018) E14.
[29] J. Blackmore, S. Shrivastava, J. Sallet, C. R. Butler, R. O. Cleveland, Ultrasound neuromodulation: A review of results, mechanisms and safety, Ultrasound in medicine & biology 45 (7) (2019) 1509–1536.
[30] R. S. Cobbold, Foundations of biomedical ultrasound, Oxford university press, 2006.
[31] T. S. Riis, T. D. Webb, J. Kubanek, Acoustic properties across the human skull, Ultrasonics 119 (2022) 106591.
[32] P. Riva-Posse, K. S. Choi, P. E. Holtzheimer, A. L. Crowell, S. J. Garlow, J. K. Rajendra, et al., A connectomic approach for subcallosal cingulate deep brain stimulation surgery: prospective targeting in treatment-resistant depression, Molecular Psychiatry 23 (2018) 843–849. doi:10.1038/mp.2017.59.
[33] S. Hameroff, M. Trakas, C. Duffield, E. Annabi, M. B. Gerace, P. Boyle, et al., Transcranial ultrasound (tus) effects on mental states: a pilot study, Brain stimulation 6 (3) (2013) 409–415.
[34] J. L. Sanguinetti, S. Hameroff, E. E. Smith, T. Sato, C. M. Daft, W. J. Tyler, et al., Transcranial focused ultrasound to the right prefrontal cortex improves mood and alters functional connectivity in humans, Frontiers in Human Neuroscience 14 (2020). doi:10.3389/fnhum. 2020.00052.
[35] S. J. Reznik, J. L. Sanguinetti, W. J. Tyler, C. Daft, J. J. Allen, A double-blind pilot study of transcranial ultrasound (tus) as a five-day intervention: Tus mitigates worry among depressed participants, Neurology Psychiatry and Brain Research 37 (2020). doi:10.1016/j. npbr.2020.06.004.
[36] R. C. Young, J. T. Biggs, V. E. Ziegler, D. A. Meyer, A Rating Scale for Mania: Reliability, Validity and Sensitivity, British Journal of Psychiatry 133 (5) (1978) 429–435. doi:10.1192/bjp.133.5.429.
URL https://www.cambridge.org/core/product/34DE3C8ED1EB65C54E87970C87BC0528
[37] A. J. Rush, C. M. Gullion, M. R. Basco, R. B. Jarrett, M. H. Trivedi, The Inventory of Depressive Symptomatology (IDS): psychometric properties., Psychological medicine 26 (3) (1996) 477–486. doi:10.1017/s0033291700035558.
[38] R. L. Spitzer, K. Kroenke, J. B. W. Williams, B. Lowe, A brief measure for assessing generalized anxiety disorder: the GAD-7., Archives of internal medicine 166 (10) (2006) 1092–1097. doi:10.1001/archinte.166.10.1092.
[39] K. Posner, G. K. Brown, B. Stanely, D. A. Brent, K. V. Yershova, M. A. Oquendo, et al., The Columbia-Suicide Severity Rating Scale: initial validity and internal consistency findings from three multisite studies with adolescents and adults, The American journal of psychiatry 168 (12) (2011) 1266–1277. doi:10.1176/appi.ajp.2011.10111704.
[40] T. Johnstone, K. S. Ores Walsh, L. L. Greischar, A. L. Alexander, A. S. Fox, R. J. Davidson, et al., Motion correction and the use of motion covariates in multiple-subject fmri analysis, Human brain mapping 27 (10) (2006) 779–788.
[41] E. A. Kaye, K. B. Pauly, Adapting MRI acoustic radiation force imaging for in vivo human brain focused ultrasound applications, Magnetic Resonance in Medicine 69 (3) (2013): 724-733.
[42] A. Manduca A, P. J. Bayly, R. L. Ehman, A. Kolipaka, T. J. Royston, I. Sack, et al., MR elastography: Principles, guidelines, and terminology, Magnetic Resonance in Medicine 85 (5) (2021) 2377–2390.

Figure/Table Legends

Figure 1: Study Design. This pilot study incorporated a double-blind, randomized, sham-controlled, cross-over design. (***A***) Overall design. Approximately 1 week after a baseline visit (not shown), the participant returned for the first stimulation visit (Day 0), where they were randomized 1:1 to the real-stimulation or sham-stimulation arm. Pre-treatment scales were collected: 6-item Hamilton Depression Rating Scale (HDRS-6) and expanded Positive and Negative Affect Schedule (PANAS-X). Each subject then participated in a 1-hour MRI session followed immediately by a 1-hour Treatment session. A post-treatment PANAS-X was completed immediately after the Treatment session. The HDRS-6 was repeated 24 hours later (Day 1). Participants returned 6 days later (Day 7) when their treatment assignment crossed over to sham or real, and the procedures of Day 0 were repeated. The HDRS-6 was repeated 24 hours and 7 days later (Day 8 and Day 14). The primary efficacy outcomes, shown at the bottom of the panel, were change in PANAS-X Sadness score on Day 0, change in HDRS-6 score from Day 0 to Day 1, and change in HDRS-6 score from Day 0 to Day 7. (***B***) Detail for Days 0 and 7. Participants who were randomized to real stimulation on Day 0 received five 1-minute trials of active ultrasonic stimulation (filled rectangles) during concurrent BOLD imaging the measure target engagement. The MRI session was followed immediately by the Treatment session, during which the subject received a series of 1-minute and 3-minute active ultrasonic stimulation trials (filled rectangles). Subjects who were randomized to the sham intervention had MRI without stimulation, followed immediately by a series of 1-minute and 3-minute sham stimulation trials (open rectangles). Continuous white noise was delivered during the MRI for both real and sham interventions. Custom designed auditory masking stimuli timed to coincide with ultrasound delivery were played via earbuds during the Treatment session for both real and sham arms. Similar protocols were repeated on Day 7 after cross-over.

Table 1: **Baseline demographic and clinical features for the intent-to-treat sample**. Diagnoses were determined with the Mini International Neuropsychiatric Interview, version 7.0. Two participants with bipolar disorder had a history of sub-threshold manic symptoms that did not meet criteria for bipolar 1 or 2 disorder. Only clearly documented failed antidepressant medication trials in the past 2 years were included. No significant differences were found between real and sham groups (all $p > 0.05$).

Figure 2: **Ultrasonic targeting and neuromodulation. (*A*)** Calculated ultrasound field produced at focus overlaid on sagittal and coronal images. The dimensions of the focus are 20.4 x 2.4 x 3.6 mm (MNI space). (***B***) Target engagement in an individual subject, assessed using concurrent blood oxygenation level dependent (BOLD) imaging. The subcallosal cingulate (SCC) was selectively deactivated: peak coordinates = [4, 20, -6], SCC small-volume-corrected $p < 0.001$ and whole-brain FWE-corrected $p < 0.001$. Display thresholds: $|t| > 4$, cluster size > 50 voxels. (***C***) SCC BOLD response from the example subject in panel ***B*** (blue) and fitted block-design model (red) are shown. BOLD signal decreased with ultrasound delivery (yellow). (***D***) Modulation of the targeted SCC region across the cohort ($n = 16$). Each symbol represents the BOLD response extracted from SCC for an individual subject. The bar shows the mean ± SEM response: $t(15) = -2.43$, $p = 0.028$, one-sample two-tailed t-test. The symbol colors indicate individual-subject results from small- volume-correction analyses (see **Supplementary Table S2**). Statistically significant deactivation was observed at the individual-subject level in 5 subjects and 1 trended toward deactivation (green). Two subjects showed a significant activation (red). In 8 subjects (blue), the modulation was not significant at the individual level.

Figure 3: **Selective deactivation of SCC.** Group analysis performed on the 12 subjects that showed a deactivation of the SCC during stimulation. The corresponding negative beta weights are shown in **Fig. 2D**. No other regions were significantly deactivated.

Figure 4: **Improvements in mood following following ultrasonic modulation of the SCC.** Immediate change in PANAS-X Sadness score with treatment for sham stimulation (n = 10) versus active stimulation (n = 8) for the per-protocol sample. The mean percentage change in Sadness was −63% in the active group versus versus −47% in the sham group. Between-group standardized effect size d = −1.15 (95%-confidence interval = [−2.24, −0.07]). *, p < 0.05. Data points indicate individual subjects. Error bars denote SEM.

Figure 5: **Improvements in depressive symptoms following ultrasonic stimulation of the SCC.** (***A***) Change in 6-item Hamilton Depression Rating Scale (HDRS-6) score 24 hours and 7 days post-treatment for the per-protocol sample. Between-group standardized effect size d = −1.08 (95%-confidence interval = [−2.11, −0.04]) at 24 hours and −0.59 (95%-confidence interval = [−1.59, 0.40]) at 7 days. Mean +/- SEM is shown. (***B***) Data from panel *A* are plotted again to show data points for individual subjects. (***C***) Data from *A* are replotted as percentage change relative to pre-treatment on Day 0. HDRS-6 scores at 1 and 7 days changed by −55% and −52% in the active group and −22% and −29% in the sham group, respectively. Mean +/- SEM is shown. (***D***) Data from *C* are plotted again to show data points for individual subjects. (***E***) The proportion of subjects who experienced ≥ 50% reduction in HDRS-6 score (response rate) is shown at 24 hours and 7 days for the active group (n = 9) and sham group (n = 10).

Table 2: **Stimulation Safety.** Twenty-four hours after ultrasonic stimulation, participants completed a standard clinical questionnaire (26) that assessed a range of potential side effects. The data are shown separately for the active (left column) and sham (right column) stimulation.

	Real Stimulation (n=10)	Sham Stimulation (n=12)	All Subjects (n=22)
Demographics			
Age, years, mean (SD)	37.37 (11.85)	41.23 (8.41)	39.47 (10.05)
Female Gender, n (%)	6 (60%)	8 (67%)	14 (64%)
Non-Hispanic White, n (%)	7 (70%)	10 (83%)	17 (77%)
Education, years, mean (SD)	15.9 (1.10)	15.83 (1.64)	15.86 (1.39)
Diagnoses and Comorbidities			
Primary DSM-5 diagnosis			
Major Depressive Disorder, n (%)	9 (90%)	11 (92%)	20 (91%)
Bipolar Disorder, n (%)	1 (10%)	1 (8%)	2 (9%)
Generalized Anxiety Disorder, n (%)	4 (40%)	7 (58%)	11 (50%)
Panic Disorder, n (%)	2 (20%)	4 (33%)	6 (27%)
Agoraphobia, n (%)	3 (30%)	1 (8%)	4 (18%)
Social Anxiety Disorder, n (%)	4 (40%)	5 (42%)	9 (41%)
Obsessive Compulsive Disorder, n (%)	2 (20%)	1 (8%)	3 (14%)
Posttraumatic Stress Disorder, n (%)	4 (40%)	2 (17%)	6 (27%)
Alcohol Use Disorder (mild), n (%)	0 (0%)	1 (8%)	1 (5%)
Other Substance Use Disorder (mild), n (%)	2 (20%)	0 (0%)	2 (9%)
Lifetime History of Psychosis, n (%)	0 (0%)	1 (8%)	1 (5%)
Severity Scales			
HDRS-6, mean (SD)	12.00 (2.91)	11.42 (1.38)	11.68 (2.17)
IDS-SR, mean (SD)	43.90 (9.80)	44.42 (9.62)	44.18 (9.47)
QIDS-SR, mean (SD)	17.10 (3.28)	18.33 (3.11)	17.77 (3.18)
YMRS, mean (SD)	1.10 (1.20)	1.00 (0.85)	1.05 (1.00)
GAD-7, mean (SD)	12.60 (5.80)	10.00 (5.38)	11.18 (5.59)
Chronicity and Resistance			
Age of Onset, years, mean (SD)	17.70 (5.25)	14.33 (5.82)	15.86 (5.70)
Duration of Current Episode, months, median (IQR)	13.00 (12.00)	24.00 (27.50)	20.00 (23.25)
Chronic Episode (>24 months), n (%)	4 (40%)	6 (50%)	10 (45%)
Failed Antidepressant Trials, Current Episode, mean (SD)	1.60 (0.70)	1.42 (1.24)	1.50 (1.01)
Maudsley Staging Method, mean (SD)	7.40 (1.58)	7.42 (1.38)	7.41 (1.44)

Table 1: **Baseline demographic and clinical features for the intent-to-treat sample**. Diagnoses were determined with the Mini International Neu- ropsychiatric Interview, version 7.0. Two participants with bipolar disorder had a history of sub-threshold manic symptoms that did not meet criteria for bipolar 1 or 2 disorder. Only clearly documented failed antidepressant medication trials in the past 2 years were included. No significant differences were found between real and sham groups (all $p > 0.05$).

	Real (N=21)					Sham (N=21)				
GASE Rating	**Not Present**	**Mild**	**Moderate**	**Severe**	**Related to Treatment? (%)**	**Not Present**	**Mild**	**Moderate**	**Severe**	**Related to Treatment? (%)**
Headache	9	9	3	0	6 (28.57)	7	8	5	1	3 (14.29)
Hair loss	21	0	0	0	0 (0)	21	0	0	0	0 (0)
Dry mouth	13	7	1	0	1 (4.76)	13	7	1	0	0 (0)
Dizziness	17	3	1	0	1 (4.76)	11	10	0	0	2 (9.52)
Chest pain	20	1	0	0	0 (0)	20	1	0	0	0 (0)
Palpitations	19	1	1	0	2 (9.52)	19	2	0	0	1 (4.76)
Breathing problems	21	0	0	0	0 (0)	20	1	0	0	0 (0)
Subjective blood circulation-associated problems	19	1	1	0	0 (0)	20	1	0	0	1 (4.76)
Abdominal pain	21	0	0	0	0 (0)	16	3	2	0	0 (0)
Nausea	19	2	0	0	0 (0)	18	2	1	0	0 (0)
Vomiting	21	0	0	0	0 (0)	21	0	0	0	0 (0)
Constipation	18	2	1	0	0 (0)	13	5	2	1	0 (0)
Diarrhea	20	1	0	0	0 (0)	17	4	0	0	0 (0)
Reduced appetite	18	2	1	0	1 (4.76)	16	5	0	0	0 (0)
Increased appetite	18	1	2	0	0 (0)	18	3	0	0	0 (0)
Difficulty urinating	21	0	0	0	0 (0)	21	0	0	0	0 (0)
Problems with sexual performance or sex organs	21	0	0	0	0 (0)	21	0	0	0	0 (0)
Painful or irregular menstruation	21	0	0	0	0 (0)	21	0	0	0	0 (0)
Skin rash or itching	20	1	0	0	0 (0)	20	1	0	0	0 (0)
Tendency to develop bruises	18	1	2	0	0 (0)	20	0	1	0	0 (0)
Fever, increased temperature	21	0	0	0	0 (0)	21	0	0	0	0 (0)
Abnormal sweating	20	0	0	1	1 (4.76)	20	1	0	0	0 (0)
Hot flashes	20	0	1	0	1 (4.76)	18	3	0	0	0 (0)
Convulsions or seizures	21	0	0	0	0 (0)	21	0	0	0	0 (0)
Fatigue, loss of energy	13	3	2	3	3 (14.28)	12	3	6	0	2 (9.52)
Tremor	19	1	1	0	0 (0)	19	2	0	0	0 (0)
Insomnia, sleeping problems	11	7	1	2	1 (4.76)	15	5	1	0	0 (0)
Nightmares or abnormal dreams	15	2	3	1	1 (4.76)	18	3	0	0	0 (0)
Back pain	14	5	1	1	1 (4.76)	14	4	3	0	1 (4.76)
Muscle pain	16	5	0	0	1 (4.76)	13	6	1	1	2 (9.52)
Joint pain	16	3	1	1	1 (4.76)	14	6	0	1	2 (9.52)
Agitation	16	3	2	0	1 (4.76)	15	4	1	1	1 (4.76)
Irritability, nervousness	12	6	2	1	2 (9.52)	11	7	2	1	1 (4.76)
Depressed mood	8	4	6	3	1 (4.76)	7	6	6	2	1 (4.76)
Thoughts about suicide	15	4	1	1	1 (4.76)	16	3	0	2	1 (4.76)
Anxiety, fearfulness	9	8	3	1	1 (4.76)	10	5	5	1	1 (4.76)

Table 2: **Stimulation Safety.** Twenty-four hours after ultrasonic stimulation, participants completed a standard clinical questionnaire (26) that assessed a range of potential side effects. The data are shown separately for the active (left column) and sham (right column) stimulation.

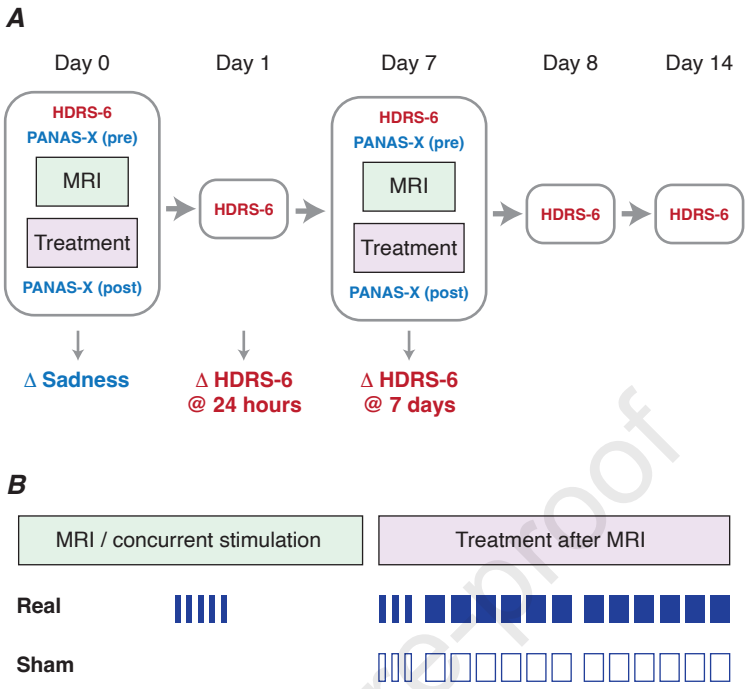

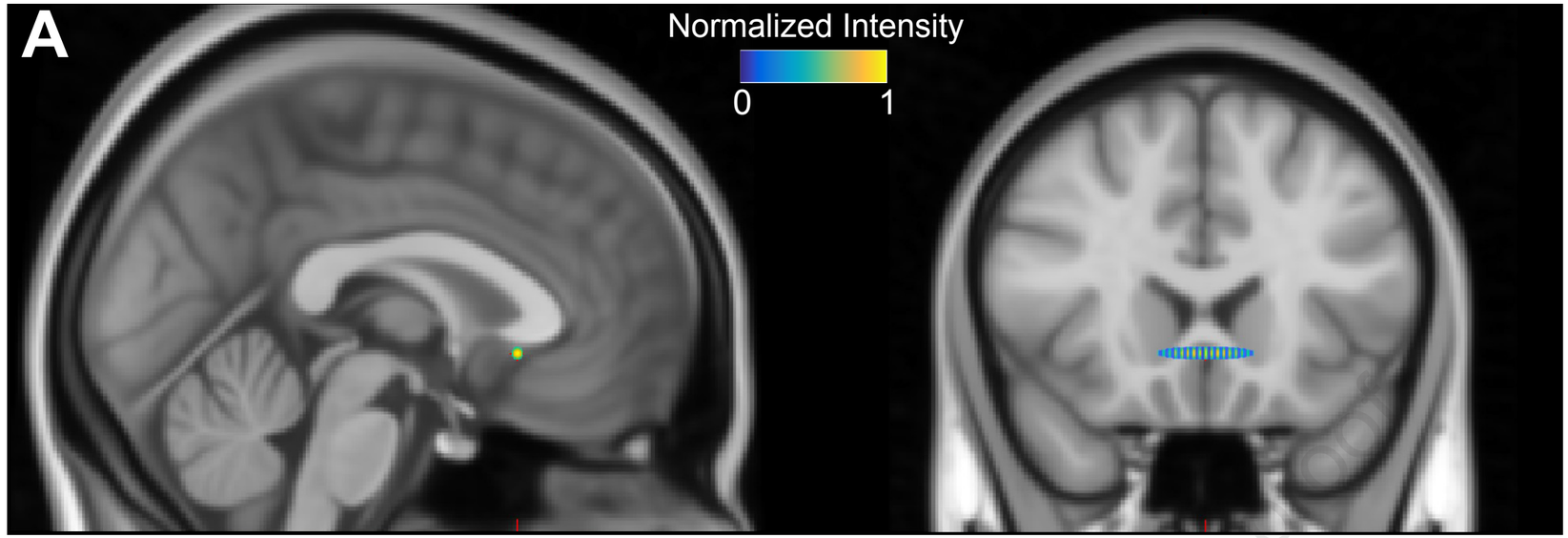
A
Normalized Intensity
0
1

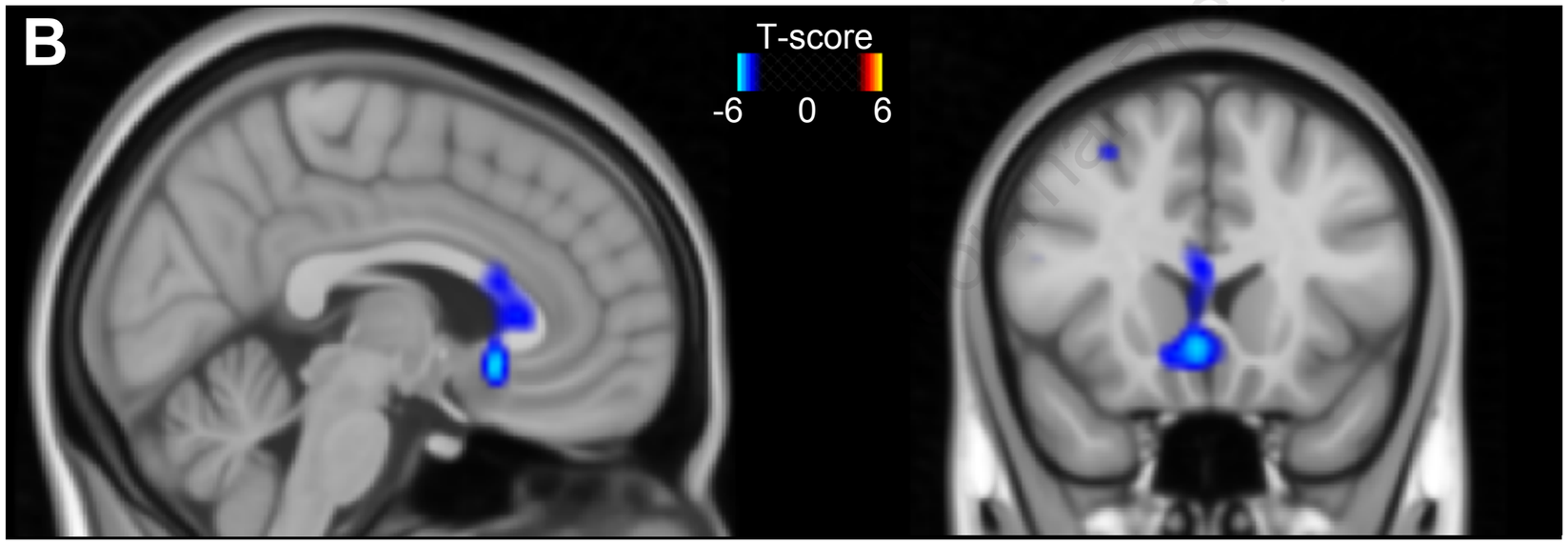
B
T-score
-6
0
6

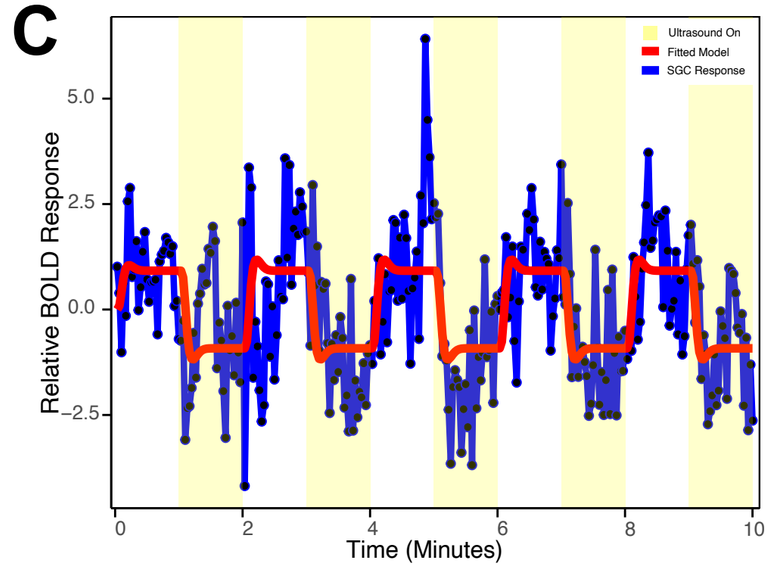
C
Ultrasound On
Fitted Model
SGC Response
Relative BOLD Response
5.0
2.5
0.0
−2.5
0
2
4
6
8
10
Time (Minutes)

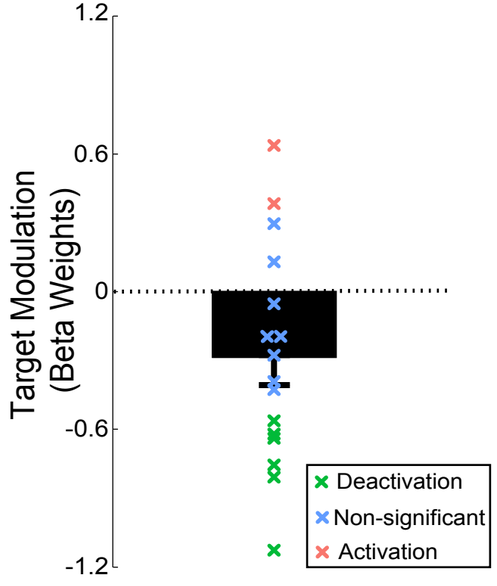
D
Target Modulation
(Beta Weights)
1.2
0.6
0
-0.6
-1.2
Deactivation
Non-significant
Activation